Preparation and Stability Study of Carboxyl Terminated Silicone Oil Modified Silicone-oil-based Ferrofluid

Qianru Zhou, Fang Chen, Ying Liu, and Jun Li*

College of Materials science and engineering, Sichuan University, Sichuan Chengdu 610065, PR China

In this study, ferrofluids were prepared by colloidal dispersion of paramagnetic Fe_3O_4 nanoparticles coated with long-chain carboxyl terminated silicone oil in silicone oil. Effect of pH value of the aqueous solution on coating was investigated. The IR and TG analysis indicated that acid conditions favored the coating of carboxyl terminated silicone oil. Stabilities of ferrofluids were characterized by density change and mass specific saturated magnetization change during centrifugation and static settlement observation. The static settlement observation indicated that the prepared silicone-oil-based ferrofluids have better stability than unmodified and oleic acid modified ferrofluids. Finally, the magnetic properties and stability of ferrofluids with different particle mass fraction were characterized.

Keywords : carboxyl terminated silicone oil, ferrofluid, stability, Fe_3O_4 nanoparticles, pH value

1. Introduction

Silicone-oil-based ferrofluids are colloidal dispersions of small single-domain magnetic particles suspended in silicone oil. Silicone oil exhibits excellent thermostability and a relatively small change in viscosity as a function of temperature. Thus, silicone-oil-based ferrofluid is an attractive choice in dynamic sealing, which can adapt to wide temperature range and extremely harsh environment [1]. The ferrofluids are required to show good stability, high saturation magnetization, high initial permeability, low viscosity and saturated vapor when using in sealings area [1]. Stability is the prerequisite for the existence of various characteristics of ferrofluids, hence it is the most important property. Stability is a measure of the ability of the particles to be kept suspended in the fluid for a long period of time, i.e. minimum agglomeration and less sedimentation. The factors affecting the stability of magnetic liquids mainly include particle size, thickness of adsorption layer, existence of surface charge, and solvation between surface layer and carrier liquid. Methods such as static observation, Gouy magnetic balance [2], ultraviolet-visible spectroscopy (UV-vis) [3], dynamic light scattering (DLS) [4] and small-angle neutron scattering (SANS) [5,

6], etc. have been used to characterize stability of ferrofluids, including water-based, hydrocarbon-oil-based, deuterated-benzene-based and decahydronaphthalene-based ferrofluids. However, few papers about silicone-oil-based ferrofluids have focused on the stability characterization.

Iron oxide nanoparticles are mostly used as magnetic particles in ferrofluids due to their high saturation magnetization and their high magnetic susceptibility [7-9]. In order to counterbalance van der Waals attraction and attractive part of magnetic dipolar interaction, colloidal stability of magnetic liquids requires an additional repulsion between the particles [10]. This may be realized through a steric hindrance by coating the particles with surfactant chains [11, 12]. Several kinds of surfactants have been used to prepare silicone-oil-based ferrofluids. Chen *et al*. used ethoxy terminated polydimethylsiloxane to modify Fe_3O_4 magnetic nanoparticles [2]. The Fe_3O_4 magnetic nanoparticles were coated with a SiO_2 layer by the hydrolysis of tetraethoxysilane. The hydrolyzed ethoxy groups of polydimethylsiloxane grafted on the silica shell through chemical bond. Wilson *et al.* synthesized carboxyl terminated silicone oil surfactant and prepared silicone-oil-based ferrofluids [13]. Hang Zheng *et al.* prepared silicone-oil-based ferrofluid with oleic acid [14]. Jong-Hee Kim *et al.* prepared silicone-oil-based ferrofluid with a silicone surfactant of α, ω-(3-aminopropyl) polydimethylsilxane [15]. Magnetic silicone fluids containing mag-

*Corresponding author: Tel: +0086-85405332
Fax: +0086-85405332, e-mail: abthonyli@163.com

netite have also been described in the patent literature [16, 17]. The relation between surfactants and stability of silicone-oil-based ferrofluids have not been researched yet. In this paper, we compared the stability of unmodified, oleic acid modified and carboxyl terminated silicone oil modified silicone-oil-based ferrofluids.
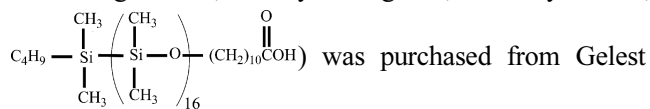
The pH value of the solution affects the surfactant coating on the nanoparticles. Mornet *et al.* carried out the reaction of anchoring the dextran corona around the magnetite/APS cores at pH 3 [18]. Fang Chen *et al.* prepared PFPE-oil-based ferrofluids when the pH of the precursor solution was 6-6.5 [19]. Wilson *et al.* reported that the PDMS stabilizers were absorbed onto the magnetite nanoparticle surfaces via the carboxylate groups in an interfacial reaction under acidic conditions [13].

In this paper, carboxyl terminated silicone oil (Product code MCR-B12) is chosen as the surfactant, considering that they have carboxylic acid anchors, which may be chemically absorbed on the nanoparticles; moreover, the tail ends could be compatible with the silicone oil. Effect of pH value of the aqueous solution on coating was investigated. The stabilities of ferrofluids were studied by density change and mass specific saturated magnetization change during centrifugation, and static settlement observation. Stable silicone-oil-based ferrofluid was prepared successfully.

2. Experimental Procedure

2.1. Raw Materials

Ferric chloride ($FeCl_3 \cdot 6H_2O$), ferrous sulfate ($FeSO_4 \cdot 7H_2O$) and sodium hydroxide were purchased from Chengdu Kelong Chemical Reagent Plant. Ethanol was purchased from Chengdu Changlian Chemical Co. Ltd. Carboxyl terminated silicone oil (Product code MCR-B12) (Molecular weight 1500, density 0.94 g/cm^3, viscosity 20 cSt,

$$C_4H_9 - \underset{\underset{CH_3}{|}}{\overset{\overset{CH_3}{|}}{Si}} - \left(\underset{\underset{CH_3}{|}}{\overset{\overset{CH_3}{|}}{Si}} - O \right)_{16} (CH_2)_{10}\overset{\overset{O}{\parallel}}{C}OH$$

) was purchased from Gelest Inc. Silicone oil was purchased from Dow Corning Inc. All chemicals are analytical grade without further purification. Deionized water was used throughout the experiments.

2.2. Preparation of silicone-oil-based ferrofluid

Fe_3O_4 nanoparticles were synthesized by co-precipitation method [20]. Briefly, 0.030 mol $FeCl_3 \cdot 6H_2O$ and 0.018 mol $FeSO_4 \cdot 7H_2O$ were dissolved in 200 mL deionized water at 70 °C. Then 0.2 mol NaOH was dissolved in 200 mL deionized water and the sodium hydroxide solution was added quickly into the iron solution under vigorous

stirring (500 rpm). The reaction last for 30 minutes and the Fe_3O_4 nanoparticles were synthesized.

To investigate the effect of pH value of the aqueous solution on the modified nanoparticles, pH value was adjusted to 2.03, 3.04, 5.02, 7.02, 9.03 respectively. The mass of adding MCR-B12 was 1.4 g. To investigate the surfactant amount on the modified nanoparticles and ferrofluid stabilities, the adding MCR-B12 amount were 1.04, 1.40, 1.74 and 2.09 g respectively when pH value of the aqueous solution was 3.04. The mixtures were vigorously stirred for 2 h at 70 °C. The resultant magnetic nanoparticles were isolated by magnet and were washed 8 times with deionized water. Then the obtained black particles were dried in vacuum at 80 °C for 8 h.

Finally, the modified Fe_3O_4 nanoparticles were dispersed in silicone oil through mechanical agitation. Stable silicone-oil-based ferrofluids were obtained.

2.3. Characterization

The pH value of solution was measured by MP511 pH meter. X-ray diffraction measurements were carried out on a DX-2700 diffractometer, using Cu Kα radiation. The modification effect of the Fe_3O_4 nanoparticles was examined by A Nicolet iS10 Fourier transform infrared spectroscopy (FT-IR). The weight loss of particles and temperature resistance of surfactants were measured by STA449F3 synchro thermal analyzer (Argon atmosphere, 25 °C-800 °C, heating rate 10 °C/min). The size and morphology of Fe_3O_4 nanoparticles was determined by JEOL JEM-2100 F transmission electron microscope (TEM). The magnetic properties of nanoparticles and ferrofluids were measured on a Lake Shore 7410 vibrating sample magnetometer (VSM). The density of the samples before and after centrifugal force was measured by a ST-300GM automatic liquid hydrometer.

3. Results and Discussion

3.1. The characterization of MCR-B12 modified magnetite nanoparticles

The XRD patterns of the uncoated and MCR-B12 coated magnetite nanoparticles are shown in Fig. 1. No obvious difference could be observed among these patterns and a series of characteristic peaks could been seen for (111), (220), (311), (400), (422), (511), (440) and (533) planes of Fe_3O_4 (PDF 19-0629) [21]. It indicates that the Fe_3O_4 nanoparticles are synthesized successfully by coprecipitation and the modification does not change the cubic crystal structure of Fe_3O_4 nanoparticles. During the experiment, it was found that the solution turned pale yellow after the coating process when pH value was 2.03, indicating that
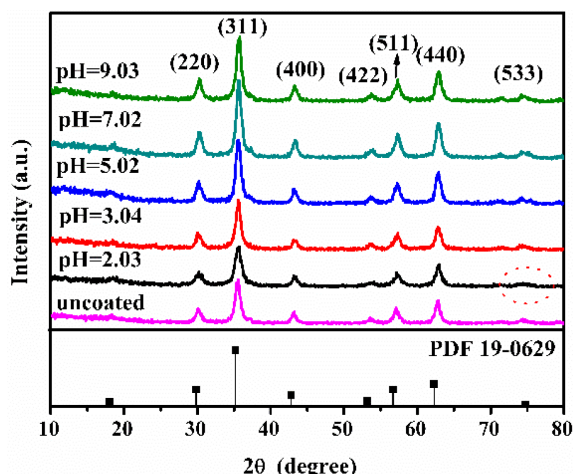
Fig. 1. (Color online) X-ray diffraction spectrum of bare Fe_3O_4 nanoparticles and the modified Fe_3O_4 nanoparticles.

Fig. 2. (Color online) FT-IR spectrum of the modified Fe_3O_4 nanoparticles (pH = 2.03, 3.04, 7.02, 9.03) and MCR-B12.

magnetite particles had been corroded and decomposed into Fe^{2+} and Fe^{3+} ions under strong acid conditions (pH = ~2). Using the Scherrer equation, the average crystalline sizes according to the main peaks are determined to be 12.51 nm and 10.69-13.12 nm for the uncoated and coated particles respectively. MCR-B12 has no diffraction peaks, thus other characterizations are needed to ensure whether the coating is successful or not.

The FT-IR spectra of the modified Fe_3O_4 nanoparticles (pH = 2.03, 3.04, 7.02, 9.03) and MCR-B12 are presented in Fig. 2. From spectra of the modified Fe_3O_4 nanoparticles, the characteristic peak around 586.62 cm^{-1} is due to the stretching vibration of the Fe-O and the -OH stretching vibrational band at 3410.03 cm^{-1} is due to the absorbed water in the sample [22]. Comparing these patterns, it can be seen that the characteristic peaks of MCR-B12 also show in the spectrum of modified Fe_3O_4 nanoparticles (pH = 3.04, 7.02, 9.03). The absorption peak at 2967.56 cm^{-1} can be ascribed to the asymmetric stretch of the CH_3 in MCR-B12. The two peaks at 1409.11 and 1248.83 cm^{-1} are due to the asymmetric vibrations of Si-CH_3. The absorption peaks at 1102.09 and 1028.34 cm^{-1} correspond to the asymmetric stretching vibration of Si-O-Si bond [23]. The peak at 807.11 cm^{-1} is attributed to the symmetric stretching vibration of Si-CH_3 bond [24]. These results clearly indicate that the MCR-B12 has been successfully grafted onto the surface of Fe_3O_4 nanoparticles. Furthermore, the C=O absorption peak of MCR-B12 is at 1714.29 cm^{-1} and the C=O absorption peak of the modified nanoparticles (pH = 3.04, 7.02, 9.03) are at 1629.60 cm^{-1}, 1605.52 cm^{-1} and 1617.56 cm^{-1} respectively, showing obvious red shift. This is caused by the reaction of -COOH and -OH (absorbed onto the magnetite
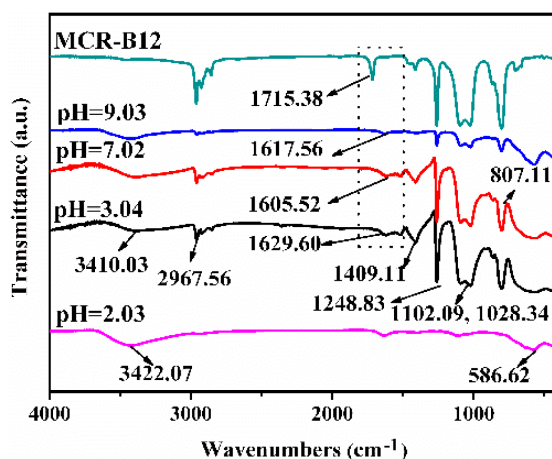
surface). The -COOH group in MCR-B12 becomes -COO^- and finally attached to the magnetite nanoparticle surface, so the modification is chemical adsorption [25]. When pH value reaches 2.03, the characteristic peaks of MCR-B12 disappear in the spectrum of modified Fe_3O_4 nanoparticles, indicating that surfactant coating isn't successful under strong acid conditions. This can be explained that it is very hard to ionize hydrogen ions for MCR-B12 when pH value reaches 2.03. The Fe_3O_4 nanoparticles are corroded and partly dissolves into Fe^{2+} and Fe^{3+} under strong acidic conditions, thus influencing the absorption of MCR-B12. It is worth noting that the stronger the acidity of the aqueous solution, the greater the absorption peak intensity, including Si-CH_3, Si-O-Si, CH_3 absorption peaks, indicating that MCR-B12 could be absorbed on the nanoparticles more easily under acidic conditions.

Figure 3 shows the TG curves of the modified Fe_3O_4 nanoparticle with different pH values and the bare Fe_3O_4 nanoparticle. Before 150 °C, the mass loss is the residual water on the surface of the nanoparticles [18]. As temperature increasing from 150 °C to 800 °C, the curve of the bare Fe_3O_4 nanoparticle barely fall. The mass loss of the modified Fe_3O_4 nanoparticle (pH = 3.04, 5.02 ,7.02) from 150 °C to 800 °C is due to the decomposition of coated MCR-B12 on the surface of the particles. The calculated amount of the absorbed MCR-B12 are 7.82 %, 10.57 % and 13.62 % when pH values are 7.02, 5.02 and 3.04 respectively. The amount of absorbed MCR-B12 is larger under acidic conditions. This can be explained that the isoelectric potential of Fe_3O_4 nanoparticles is about 6.8 [26] and the surface of Fe_3O_4 nanoparticles owns larger positive electricity under acidic conditions, thus the electrostatic attraction between -COO^- and Fe_3O_4 nanoparticles is stronger, leading to the increase of absorbed MCR-B12
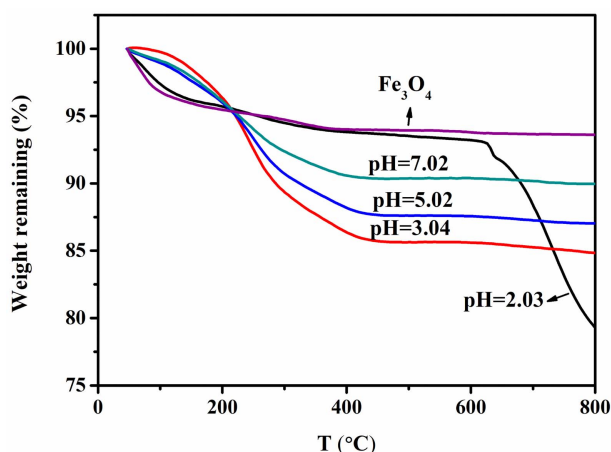
Fig. 3. (Color online) TG curves of the modified Fe_3O_4 nanoparticles (pH = 2.03, 3.04, 5.02, 7.02) and bare Fe_3O_4 nanoparticle.

Fig. 4. (Color online) TEM images and size distribution histograms of bare Fe_3O_4 magnetic nanoparticles (a, c), modified Fe_3O_4 magnetic nanoparticles (pH = 3.04, $m_{MCR-B12}$ = 1.74 g) (b, d) and a HRTEM image of a single modified particle (e).

amount. But when pH value of aqueous solution reaches 2.03, the curve has hardly changed from 150 °C to 600 °C, further confirming the surfactant is not coated successfully, consistent with the IR analysis. The reason for the sudden decline of the curve at 600 °C may be the decreased temperature resistance of corroded nanoparticles. Additionally, when pH value is 3.04, the modified particles after drying and grinding are black. When pH value is 5.02 and 7.02, the modified particles turn a little brownish red. This is due to that the absorbed MCR-B12 amount is not enough to coat the Fe_3O_4 nanoparticles completely and Fe_3O_4 nanoparticles are partly oxidized [14]. When pH value reaches 2.03, the modified particles turn brownish red completely, which can be explained that surfactant coating process is not successful and Fe_3O_4 nanoparticles were severely oxidized. To conclude, the acid condition favors coating of MCR-B12.

TEM images and size distribution histograms of bare Fe_3O_4 magnetic nanoparticles (a, c) and modified Fe_3O_4 magnetic nanoparticles (pH = 3.04, $m_{MCR-B12}$ = 1.74 g) (b, d) and a HRTEM image of a single modified particle (e) are shown in Fig. 4. The bare Fe_3O_4 magnetic nanoparticles exhibit serious aggregation and most particles are irregular quadrilateral in Fig. 4(a). This is due to that both large specific surface area and attraction between magnetic dipoles lead to bare Fe_3O_4 magnetic nanoparticles spontaneous aggregation. However, the modified Fe_3O_4 magnetic nanoparticles are homogeneously dispersed without flocculation, globular shaped and clear boundary as shown in Fig. 4(b). For particle sizes, bare Fe_3O_4 magnetic nanoparticles range from 6 nm to 19 nm as shown in Fig. 4(c) and the mean size is 11.56 nm. The modified Fe_3O_4 magnetic nanoparticles are in narrower
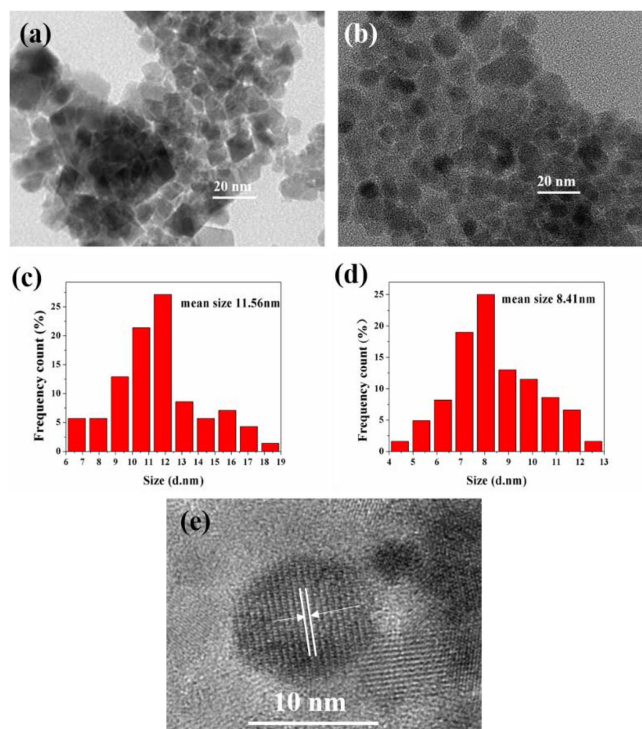
distribution ranging from 4 nm to 13 nm as shown in Fig. 4(d) and the mean size of the modified Fe_3O_4 magnetic nanoparticles is smaller, 8.41 nm. This can be explained that MCR-B12 restricted the growth of Fe_3O_4 nanoparticles by firm chemical adsorption on the surface and also prevented particles agglomeration by steric hindrance of MCR-B12 long chains [27]. Fig. 4(e) is a HRTEM image of a single modified particle with an interplanar spacing of about 0.48 nm corresponding to lattice fringe (111) of Fe_3O_4, further demonstrating the crystal structure of the Fe_3O_4 particles. The lattice fringes demonstrate that highly monocrystalline Fe_3O_4 nanoparticles were formed. Additionally, the average particle sizes are almost consistent with the average crystalline sizes according to the Scherrer equation.

Figure 5 shows the magnetic hysteresis curves of the bare Fe_3O_4 nanoparticles (a) and the modified particles with different MCR-B12 adding amount 1.04 g (b), 1.40 g (c), 1.74 g (d) and 2.09 g (e) when pH value was 3.04, in which the nanoparticles exhibit superparamagnetic behavior, with no hysteresis. It can be seen that the mass specific saturated magnetization of bare Fe_3O_4 nanoparticles is 69.98 emu/g, which is obviously lower than that of bulk Fe_3O_4 (90 emu/g). This phenomenon may be
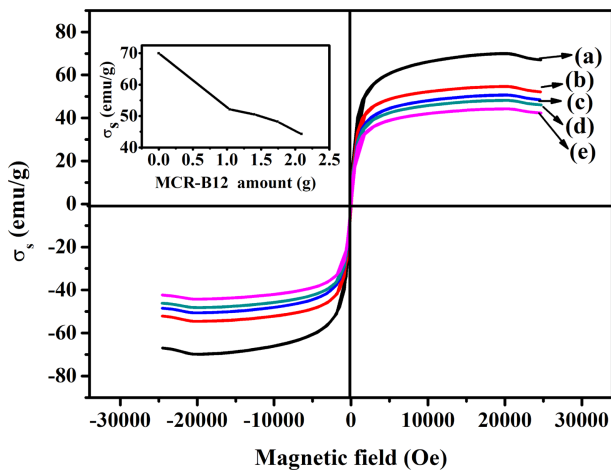
Fig. 5. (Color online) Magnetic hysteresis curves of the bare Fe_3O_4 nanoparticles (a) and the modified particles with different MCR-B12 adding amount: (b) $m_{MCR-B12}$ = 1.04 g. (c) $m_{MCR-B12}$ = 1. 40 g. (d) $m_{MCR-B12}$ = 1.74 g. (e) $m_{MCR-B12}$ = 2.09 g.

attributed to the small particle size effect since a non-collinear spin arrangement occurs primarily at or near the surface, which results in the reduction of magnetic moment in Fe_3O_4 nanoparticles [28]. The mass specific saturated magnetization of the prepared Fe_3O_4 nanoparticles are higher than the reported mass specific saturated magnetization of Fe_3O_4 nanoparticles in some republished literatures [29, 30]. This can be explained that the magnetic properties of the magnetic nanoparticles are related to the crystallinity [31]. According to the sharp diffraction peaks by XRD and the HRTEM image, the prepared Fe_3O_4 nanoparticles exhibit good crystallinity. The well-crystallized particles have a thinner non-magnetic surface layer and the less superparamagnetic relaxation [32]. Better crystallinity in Fe_3O_4 nanoparticles would also result in less crystal defects [32]. Therefore, the superexchange interaction of Fe-O-Fe was strengthened, and the magnetic properties of Fe_3O_4 nanoparticles were improved. Additionally, the modification reduced σ_s from 69.98 emu/g (uncoated Fe_3O_4 magnetic nanoparticles) to 48.22 emu/g ($m_{MCR-B12}$ = 1.74 g), which can be explained by two reasons. Firstly, MCR-B12 as a non-magnetic material lowered magnetization per unit mass. Secondly, this could also be attributed to the surface spin effect of Fe_3O_4 nanoparticles caused by modification [28]. Mass specific saturated magnetization of the modified particles decrease with the increasing MCR-B12 adding amount. This indicates that the surface of Fe_3O_4 magnetic nanoparticles has enough active binding sites when pH value of solution was 3.04 and physical adsorption may exist.

3.2. The characterization of stability of silicone-oil-based ferrofluids

The presence of surfactants layers in ferrofluids is known to lead to an increase in the average distance between particles and, correspondingly, the weakening of the magnetic dipole-dipole attraction. One of the most important factors affecting ferrofluid stability is the concentration of surfactant molecules in solution [5]. In practice, there is an optimal ratio of the contents of magnetic nanoparticles and surfactant, a deviation from which violates ferrofluid stability [6, 7, 33].

The density of ferrofluid with 10 % particle mass fraction before and after centrifugation when the MCR-B12 addition were 1.04, 1.40, 1.74 and 2.09 g respectively are given in Fig. 6. The particle mass fraction of ferrofluids is defined as the mass of the magnetic particles as a percentage of the mass of the ferrofluids. The difference between ρ_{after} and ρ_{before} increased first and then decreased with the MCR-B12 amount. When the surfactant amount is too small, the Fe_3O_4 nanoparticles can't be completely coated by the surfactant, thus the space impedance between the particles is insufficient to resist the attraction between the particles. However, too much dosage of surfactant can result in adhesion between particles thus leading to settlement. In conclusion, the best amount of MCR-B12 was 1.74 g for stability of silicone-oil-based ferrofluid and $\rho_{after}/\rho_{before}$ of ferrofluid was 98.204 %.

Comparing the stabilities of the unmodified (a), oleic acid modified (b) and MCR-B12 modified (c) silicone-oil-based ferrofluids, optical images of these ferrofluids under gravity for 7 days and 14 days are displayed in Fig. 7. The unmodified ferrofluids (a) turned red after 7 days, which was due to the oxidation of Fe_3O_4 nanoparticles. The oleic acid modified (b) and MCR-B12 modified (c)
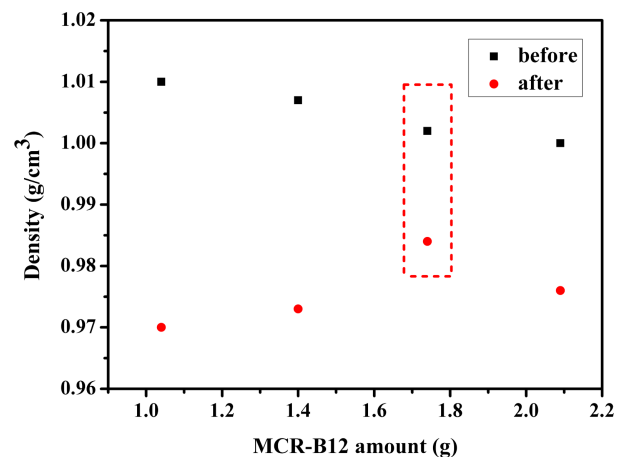

Fig. 6. (Color online) The density of ferrofluid with different MCR-B12 adding amount before and after centrifugation.
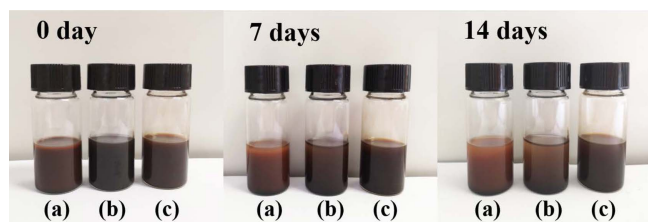
Fig. 7. (Color online) Unmodified (a), oleic acid modified (b) and MCR-B12 modified (c) silicone-oil-based ferrofluids under gravity for 7 days and 14 days.

silicone-oil-based ferrofluids remained black after 7 days, confirming that surfactant had coated the magnetite nanoparticles successfully and weakened the oxidation. In addition, color of the upper ferrofluids (a) and (b) turned obviously shallower after 14 days. This indicated that the unmodified ferrofluid and oleic acid modified ferrofluid both exhibited serious particle sedimentation under gravity. From the slight color change of the upper ferrofluids (c), MCR-B12 modified silicone-oil-based ferrofluids exhibited best stability. The absorbed MCR-B12 layers effectively counterbalances the van der Waals attraction and attractive part of magnetic dipolar interaction, thus improving the colloidal stability of ferrofluids. Additionally, MCR-B12 was more effective than oleic acid, which can be ascribed to MCR-B12 molecular chain is similar to silicone oil and has good compatibility with the carrier liquid [2, 13, 17].

3.3. Stability and Magnetic properties of the silicone-oil-based ferrofluids with different particle mass fraction

The stabilities of silicone-oil-based ferrofluids with different particle mass fraction were investigated. Fig. 8 presents the density of ferrofluids with different particle mass fraction before and after centrifugation. The difference between density before and after centrifugation increases with the particle mass fraction, which indicates the stability of ferrofluids decreases with the increasing particle mass fraction. The decline is chiefly attributed to that the increasing interparticle interaction with the particle mass fraction presses the surfactant tails in the layer closer against the magnetite surface, thus leading to particle agglomeration [34]. When particle mass fraction increases from 30 % to 40 %, the thickness of the surfactant layer decreases significantly [35]. This also points to the interlacing of surfactant tails in the layer caused by the interparticle interaction. Additionally, it is difficult to disperse the particles evenly into the silicone oil when the particle mass fraction reaches 30 %-40 %.

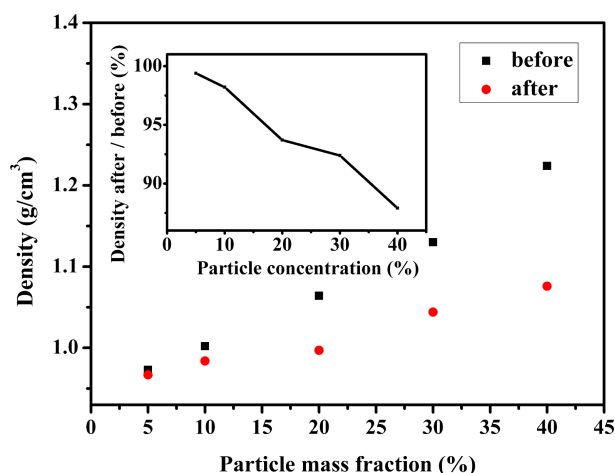The magnetic properties of ferrofluids are closely related

Fig. 8. (Color online) The density of ferrofluid with different mass fraction of particle before and after centrifugation.

to stabilities [19]. Fig. 9 shows the σ_s of the top layers of ferrofluids with different mass fraction before and after centrifugation. Silicone-oil-based ferrofluids with 5 %, 10 %, 20 %, 30 % and 40 % particle mass fraction displayed a mass specific saturated magnetization of 0.75, 2.06, 4.27, 7.26, 10.99 emu/g before centrifugation and 0.65, 1.64, 3.08, 4.75, 6.13 emu/g after centrifugation. The σ_s of the ferrofluids increases with the particle mass fraction. After centrifugation, the σ_s of the top layers of ferrofluids decreases. The centrifugation force can destroy the interaction between the magnetic particles and surfactants, thus the magnetic nanoparticles tend to agglomerate and settle [10]. After centrifugation, the large particles and aggregates in ferrofluids deposit at the bottom of the centrifuge tube, and the σ_s of the top layers of ferrofluids
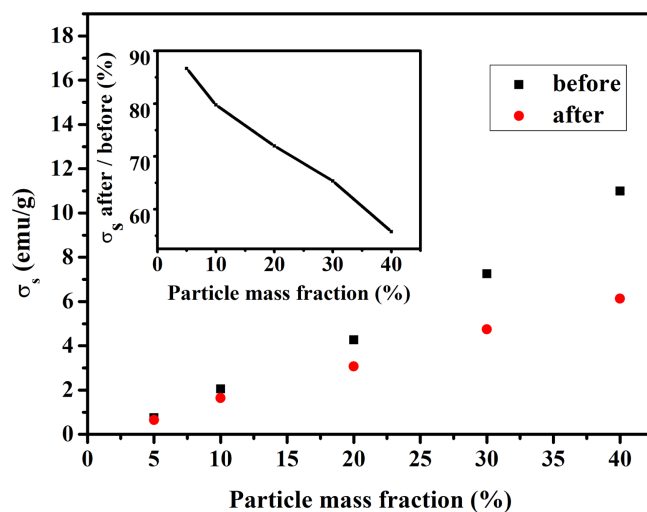

Fig. 9. (Color online) The mass specific saturated magnetization of the top layers of ferrofluids with different mass fraction before and after centrifugation.

decrease correspondingly. When ferrofluid is unstable, the particle subsidence is quite serious and the magnetic property of the top layer of ferrofluids decreases greatly. Thus, the stability can be characterized by the change of magnetic properties of the top layer of ferrofluids. The difference between σ_s before and after centrifugation increases with the particle mass fraction, from the inset, σ_s after/before centrifugation decreases with the increasing particle mass fraction. These results indicate that the sedimentation of particles is more serious and the stabilities of ferrofluids decrease with the increasing particle mass fraction, consistent with density change analysis. In practical dynamic sealings, magnetic properties and stability of ferrofluids both have great influence on sealing effects. There must be a balance between magnetic properties and stability for ferrofluids, and the sealing effect may be the best.

4. Conclusions

In this study, ferrofluid was prepared by colloidal dispersion of paramagnetic Fe_3O_4 nanoparticles coated with long-chain carboxyl terminated silicone oil (MCR-B12) in silicone oil. MCR-B12 is absorbed onto the surface of Fe_3O_4 magnetic nanoparticles through chemical bonds and the modified Fe_3O_4 magnetic nanoparticles are globular shaped and monodisperse whose particle size are in a narrow distribution (4-13 nm). TG analysis indicates that acidic conditions favors the MCR-B12 coating. When the mass of MCR-B12 was 1.74 g, the obtained silicone-oil-based ferrofluid were most stable. The digital photographs indicate that ferrofluids have better stability than unmodified ferrofluids and oleic acid modified ferrofluids. The magnetic properties of ferrofluids increase with the particle mass fraction, however, the sedimentation of particles is more serious and the stabilities of ferrofluids decrease with the increasing particle mass fraction. In practical dynamic sealings, there must be a balance between magnetic properties and stability for ferrofluids, and the sealing effect may be the best.

Acknowledgments

References

[1] R. Moskowitz, A S L E Transactions **18**, 135 (1975).
[2] H. J. Chen, Y. M. Wang, J. M. Qu, R. Y. Hong, and H. Z. Li, Appl. Surf. Sci. **257**, 10802 (2011).
[3] H. G. Cha, W. K. Chang, S. W. Kang, B. K. Kim, and Y. S. Kang, J. Phys. Chem. C **114**, 9802 (2010).
[4] X. L. Liu, H. M. Fan, J. B. Yi, Y. Yang, E. S. G. Choo, J. M. Xue, D. D. Fan, and J. Ding, J. Mater. Chem. **22**, 8235 (2012).
[5] V. I. Petrenko, M. V. Avdeev, L. A. Bulavin, L. Almasy, N. A. Grigoryeva, and V. L. Aksenov, Crystallogr. Rep+. **61**, 121 (2016).
[6] V. I. Petrenko, M. V. Avdeev, V. L. Aksenov, L. A. Bulavin, and L. Rosta, J. Surf. Investig. X-Ray Synchro. **3**, 161 (2009).
[7] Rosensweig and RonaldE, Ferrohydrodynamics, Cambridge University Press (1985) pp 344.
[8] S. Odenbach, Ferrofluids. Magnetically Controllable Fluids and their Applications, Springer-Verlag, Berlin, Germany (2002).
[9] S. Odenbach, Colloid Surf. A-Physicochem. Eng. Asp. **217**, 171 (2003).
[10] S. Genc and B. Derin, Curr. Opin. Chem. Eng. **3**, 118 (2014).
[11] L. A. Harris, J. D. Goff, A. Y. Carmichael, J. S. Riffle, J. J. Harburn, T. G. St. Pierre, and M. Saunders, Chem. Mat. **15**, 1367 (2003).
[12] H. Pardoe, W. Chua-anusorn, T. G. St. Pierre, and J. Dobson, J. Magn. Magn. Mater. **225**, 41 (2001).
[13] K. S. Wilson, J. D. Goff, J. S. Riffle, L. A. Harris, and T. G. St Pierre, Polym. Adv. Technol. **16**, 200 (2005).
[14] H. Zheng, H. P. Shao, T. Lin, Z. F. Zhao, and Z. M. Guo, Rare Metals **37**, 803 (2016).
[15] J.-H. Kim, K.-B. Park, and K.-S. Kim, Composites Research **30**, 41 (2017).
[16] M. S. Chagnon, Stable ferrofluid compositions and method of making same, US 4356098 (1982).
[17] K. Raj, R. E. Rosensweig, and L. M. Aziz, Stable polysiloxane ferrofluid compositions and method of making same, US 58514416A (1998).
[18] S. Mornet, J. Portier, and E. Duguet, J. Magn. Magn. Mater. **293**, 127 (2005).
[19] F. Chen, Y. Liu, and Z. Q. Yan, Chem. Phys. **513**, 67 (2018).
[20] L. Peng, P. F. Qin, M. Lei, Q. R. Zeng, H. J. Song, J. Yang, J. H. Shao, B. H. Liao, and J. D. Gu, J. Hazard. Mater. **209**, 193 (2012).
[21] J. Liu, Y. Z. Bin, and M. Matsuo, J. Phys. Chem. C **116**, 134 (2012).
[22] H. C. Cui, D. C. Li, and Z. L. Zhang, Mater. Lett. **143**, 38 (2015).
[23] E. L. Zhang, C. M. Zou, and S. Y. Zeng, Surf. Coat. Technol. **203**, 1075 (2009).
[24] C. H. Huang, N. F. Wang, Y. Z. Tsai, C. C. Liu, C. I. Hung, and M. P. Houng, Mater. Chem. Phys. **110**, 299 (2008).
[25] D. Maity and D. C. Agrawal, J. Magn. Magn. Mater. **308**, 46 (2007).
[26] P. H. Tewari and A. W. Mclean, J. Colloid Interface Sci.

40, 267 (1972).

[27] H. T. Zhao, R. P. Liu, Q. Zhang, and Q. Wang, Mater. Res. Bull. **75**, 172 (2016).

[28] S. F. Si, C. H. Li, X. Wang, D. P. Yu, A. Q. Peng, and Y. D. Li, Cryst. Growth Des. **5**, 391 (2005).

[29] H. N. Meng, Z. Z. Zhang, F. X. Zhao, T. Qiu, and J. D. Yang, Appl. Surf. Sci. **280**, 679 (2013).

[30] H. Iida, K. Takayanagi, T. Nakanishi, and T. Osaka, J. Colloid Interface Sci. **314**, 274 (2007).

[31] X. Y. Qi, B. J. Stadler, J. H. Judy, and R. H. Victora, J. Appl. Phys. **93**, 7849 (2003).

[32] J. Wang, K. Zhang, Z. M. Peng, and Q. W. Chen, J. Cryst. Growth. **266**, 500 (2004).

[33] L. Vékás, M. V. Avdeev, and D. Bica, Magnetic Nanofluids: Synthesis and Structure, Springer Berlin Heidelberg (2009).

[34] V. Aksenov, M. Avdeev, M. Balasoiu, L. Rosta, G. Török, L. Vekas, D. Bica, V. Garamus, and J. Kohlbrecher, Appl. Phys. A-Mater. Sci. Process. **74**, s943 (2002).

[35] M. Avdeev, M. Balasoiu, G. Torok, D. Bica, L. Rosta, V. L. Aksenov, and L. Vekas, J. Magn. Magn. Mater. **252**, 86 (2002).